

Efficient quantum measurement of Pauli operators

Ophelia Crawford,^{1,*} Barnaby van Straaten,^{1,*} Daochen Wang,^{1,2,*} Thomas Parks,¹ Earl Campbell,^{1,3} and Stephen Brierley¹

¹Riverlane, Cambridge, UK

²Joint Center for Quantum Information and Computer Science, University of Maryland, College Park, USA

³Department of Physics and Astronomy, University of Sheffield, Sheffield, UK

Estimating the expectation value of an observable is a fundamental task in quantum computation. Unfortunately, it is often impossible to obtain such estimates directly, as the computer is restricted to measuring in a fixed computational basis. One common solution splits the observable into a weighted sum of Pauli operators and measures each separately, at the cost of many measurements. An improved version first groups mutually commuting Pauli operators together and then measures all operators within each group simultaneously. The effectiveness of this depends on two factors. First, to enable simultaneous measurement, circuits are required to rotate each group to the computational basis. In our work, we present two efficient circuit constructions that suitably rotate any group of k commuting n -qubit Pauli operators using at most $kn - k(k+1)/2$ and $O(kn/\log k)$ two-qubit gates respectively. Second, metrics that justifiably measure the effectiveness of a grouping are required. In our work, we propose two natural metrics that operate under the assumption that measurements are distributed optimally among groups. Motivated by our new metrics, we introduce SORTED INSERTION, a grouping strategy that is explicitly aware of the weighting of each Pauli operator in the observable. Our methods are numerically illustrated in the context of the Variational Quantum Eigensolver, where the observables in question are molecular Hamiltonians. As measured by our metrics, SORTED INSERTION outperforms four conventional greedy colouring algorithms that seek the minimum number of groups.

I. INTRODUCTION

Estimating the expectation value $\langle O \rangle_\psi$ of an observable O on a quantum state $|\psi\rangle$ is a fundamental task in quantum mechanical experiments. However, often there is no natural way to measure O directly and some indirect protocol is required. In particular, this is true of current quantum computers that can only measure each qubit in the computational basis defined, by convention, as eigenstates of the Pauli- Z operator.

One naive protocol, therefore, is to decompose O into a weighted sum of t Pauli operators (or Paulis) $\{P_i\}_{i=1}^t$ and then measure each P_i separately. An extended version assembles the Paulis into N commuting subsets, or “groups”, given by

$$\mathcal{C}_i := \{P_{ij}\}_{j=1}^{m_i}, \quad i = 1, \dots, N, \quad (1)$$

for some m_i . All Paulis in a group can then be measured at the same time, as any set \mathcal{C}_j of commuting Paulis can be simultaneously diagonalised by a single unitary U , so

$$\langle P \rangle_\psi = \langle \Lambda(P) \rangle_{U\psi}, \quad \text{for all } P \in \mathcal{C}_j, \quad (2)$$

where $\Lambda(P) := UPU^\dagger$ is diagonal in the computational basis. To measure all operators in \mathcal{C}_j simultaneously, we first apply the unitary “rotation” U to $|\psi\rangle$, then measure in the computational basis which yields a bitstring, z , of measurements on each qubit, and finally, for each $P \in \mathcal{C}_j$, classically post-process z according to $\Lambda(P)$ to infer $\langle P \rangle_\psi$.

Expectation estimation features prominently as the quantum sub-routine of the Variational Quantum Eigensolver (VQE) algorithm [1], which has emerged as a leading candidate for exhibiting quantum advantage in the Noisy Inter-

mediate Scale Quantum era [2]. VQE is a hybrid quantum-classical algorithm designed to find the ground state [1, 3–9], or energy spectra [10–15], of a physical or chemical system. The observable O in question is a Hamiltonian H on n qubits. In the context of quantum chemistry, H readily decomposes into a weighted sum of Paulis via, for example, the Jordan-Wigner [16], Bravyi-Kitaev [17], or Verstraete-Cirac [18] transformations.

The paper that introduced VQE [1] proposed measuring H according to the naive protocol above. However, this can be inefficient. For example, a second-quantised chemical Hamiltonian on n qubits decomposes into a very large number of Paulis that scales as n^4 . To remedy this problem, McClean *et al.* [3] proposed the extended protocol. The authors also argued using a toy example that, due to covariances between Paulis, optimally grouping \mathcal{C}_j might not be the same as minimising the number of groups, N . However, Ref. [3] did not propose strategies to obtain the commuting groups \mathcal{C}_j , neither did it show how to construct the rotation U that enables simultaneous measurement.

Recently, a series of papers [19–23] [24] have appeared that together make good progress on both the grouping strategy and rotation construction problems. Our paper is in this same arena and attacks *both* problems.

First, we contribute two new methods for constructing Clifford rotation circuits U that enable simultaneous measurement of arbitrary \mathcal{C}_j , i.e., a group containing arbitrary commuting Paulis. Like Ref. [23], we approached the problem via the stabiliser formalism but have gone further to consider the case when \mathcal{C}_j has any number $k \leq n$ of independent Paulis. We show that the number of two-qubit gates in U can be reduced in a way that scales with k . This is important because it is atypical for actual groupings to have exactly $k = n$ independent Paulis and reducing the number of two-qubit gates is important, especially in the near-term [25–39]. As far as we are aware, ours is the first paper to consider the $k < n$ case ex-

* These authors contributed equally to this work.

plicity. Also, we emphasise the role classical post-processing can play in saving quantum resources.

More specifically, we introduce constructions ‘‘CZ’’ and ‘‘CNOT’’. The CZ-construction builds on work by Van den Nest, Dehaene, and De Moor [40] in the graph-state literature to yield U with a number of two-qubit gates, or ‘‘ $2q$ -size’’, at most

$$u_{cz}(k, n) = kn - k(k + 1)/2. \quad (3)$$

The CNOT-construction builds on our CZ-construction, and work by Aaronson and Gottesman [41] and Patel, Markov, and Hayes [42] to yield U with $2q$ -size at most

$$u_{cnot}(k, n) = O(kn/\log k). \quad (4)$$

We stress that u_{cnot} and u_{cz} are worst-case upper bounds. In practice, numerical simulations are needed to determine whether the CZ- or CNOT-construction is actually more efficient. We note that, in the case of $k = n$, our methods produce a two-qubit gate count scaling no worse than the previous best of $O(n^2)$ [23]. Other works, such as Ref. [20, Appendix A], prove only that a Clifford U exists, or demonstrate a worst-case gate count scaling that is worse than $O(n^2)$ [21, Appendix B], or present a method that cannot be used for arbitrary \mathcal{C}_j [22].

When considering the grouping strategy problem, we contribute two new but natural metrics, R and \hat{R} , that quantify the performance of any given grouping. R and \hat{R} measure the ratio between the number of measurements required in the ungrouped case versus the grouped case to attain a fixed level of accuracy. The key novelty in these two metrics is that they assume measurements on the groups are distributed optimally to maximise accuracy, following Refs. [8, 43, 44]. The difference between them is that R is state-dependent but \hat{R} is designed to approximate $\mathbb{E}[R]$ over the uniform spherical measure. Therefore, R is more suitable for use given some knowledge of the underlying state $|\psi\rangle$, while \hat{R} is more suitable otherwise.

We find it useful to prove that, for all $|\psi\rangle$, breaking a single commuting group into two never improves R nor \hat{R} . More formally, let group $\mathcal{C}_{a \cup b}$ be the disjoint union of groups \mathcal{C}_a and \mathcal{C}_b ; then

$$R(\{\mathcal{C}_a, \mathcal{C}_b\}) \geq R(\{\mathcal{C}_{a \cup b}\}) \quad \text{for all } |\psi\rangle. \quad (5)$$

This result is in direct contrast to the conclusion of the aforementioned toy example used by McClean *et al.* [3], and analysed in full in Ref. [23, Sec. 10.1], that breaking a group can be advantageous. The reason for the discrepancy is that we assume measurements are distributed optimally, whereas they assume measurements are distributed uniformly.

Informed by the mathematical form of \hat{R} , we contribute our new grouping strategy SORTED INSERTION. Unlike strategies used previously [19, 20, 23], SORTED INSERTION is explicitly aware of the coefficients in the Pauli decomposition of an observable O . We present data showing SORTED INSERTION outperforming all four conventional

greedy colouring algorithms that we tried, as measured by the metric \hat{R} . Our data also *challenges* the assumption that minimising the number of groups N is optimal, as groupings with the smallest number of groups do not typically perform the best with respect to \hat{R} . Note that this does not logically contradict Eq. (5). We quantify the performance of SORTED INSERTION using the metric \hat{R} for molecules ranging in size from hydrogen H_2 , which requires two qubits, to hydrogen selenide H_2Se , which requires 38, finding that it leads to a 10 to 60 fold improvement in the number of measurements required. Note that we are defining a single measurement to consist of a measurement of all qubits, and so the number of measurements equals the number of ansatz state preparations.

Finally, we run SORTED INSERTION alongside our CZ-construction on molecules requiring up to 38 qubits to calculate the actual number of two-qubit gates required for real molecular systems. Our numerical results show that the typical number of two-qubit gates is fewer than the worst-case $u_{cz}(k, n)$ by a factor of 3.5.

II. ROTATION CONSTRUCTIONS

In this section, we assume familiarity of the reader with the stabiliser formalism, especially the $2n$ -bit binary representation of n -qubit Paulis [41, 45–47]. We follow the convention that the upper and lower halves of the binary matrix encode Z and X operators respectively. This representation is reviewed in Appendix A. We also reserve symbols I_m and 0_m for the $m \times m$ identity and all-zero matrices respectively.

Our starting point is a commuting group, S'_{start} , of m Paulis which can be represented as a binary $2n \times m$ matrix S'_{start} . By Gaussian elimination on S'_{start} , we can form a $2n \times k$ matrix S_{start} representing a set S_{start} of k independent Paulis drawn from S'_{start} where $k \leq \min(n, m)$. Our goal is to transform S_{start} , using certain allowed transformations, into a $2n \times n$ matrix S_{end} where

$$S_{\text{end}} = \begin{pmatrix} I_n \\ 0_n \end{pmatrix}. \quad (6)$$

Let U denote the circuit consisting of $1q$ and $2q$ transformations in the order they were applied from $S_{\text{start}} \rightarrow S_{\text{end}}$. Then applying U to any state $|\psi\rangle$, measuring in the computational basis, and classically post-processing allows us to measure S'_{start} on $|\psi\rangle$ simultaneously.

The allowed set \mathcal{T} of transformations on a binary $2n \times m$ matrix S is, where p ranges over all columns, r ranges over all rows, and addition is mod 2:

1. $1q$ and $2q$, one- and two-qubit quantum row operations, specifically:

- CZ on qubits i and j :

$$S_{ip} \leftarrow S_{ip} + S_{j+n,p},$$

$$S_{jp} \leftarrow S_{jp} + S_{i+n,p}.$$
- CNOT on control-qubit i and target-qubit j :

$$S_{ip} \leftarrow S_{ip} + S_{jp},$$

$$S_{j+n,p} \leftarrow S_{j+n,p} + S_{i+n,p}.$$

- HADAMARD (H) on qubit i :
 $S_{ip} \leftrightarrow S_{i+n,p}$.
 - PHASE (P) on qubit i :
 $S_{ip} \leftarrow S_{ip} + S_{i+n,p}$.
2. *cpp*, classical post-processing:
- Products of eventual single-qubit computational-basis measurements:
right-multiply by invertible $m \times m$ matrix.
 - Relabelling of qubits i and j :
 $S_{ip} \leftrightarrow S_{jp}$,
 $S_{n+i,p} \leftrightarrow S_{n+j,p}$.
3. *ext*, basis extension.
- Addition of further stabiliser:
append new column $S_{r,m+1}$.

In the near term, operations in \mathcal{T} have different costs that can be justifiably ranked as “ $2q \gg 1q > cpp > ext = 0$ ”. In the first inequality, cost can refer to either fidelity or gate-time [25–39]. Therefore, we have aimed to minimise the number of two-qubit gates, or “2q-size”, in the U resulting from our constructions. This means, for example, we never perform the *cpp* row swap using a two-qubit SWAP.

In presenting our constructions, we shall refer to the commutativity condition, preserved under \mathcal{T} , given by

$$S^T J_{2n} S = 0_n, \quad (7)$$

where S is the $2n \times m$ matrix encoding the Paulis and

$$J_{2n} = \begin{pmatrix} 0_n & I_n \\ I_n & 0_n \end{pmatrix}. \quad (8)$$

We ignore any changes in sign of stabilisers under \mathcal{T} as this can be easily accounted for by classical post-processing. Readers interested in this and other details are referred to Appendix B, where we work through our CZ-construction with a specific example.

A. CZ-construction

Important to our first approach is the special class of stabiliser states known as graph states. Consider any graph G on n vertices. The graph state $|\Phi_G\rangle$ is then defined by n independent stabiliser generators

$$g_i = X_i \prod_{j \in \text{nbd}(i)} Z_j, \quad i = 1, \dots, n, \quad (9)$$

where $\text{nbd}(i)$ is the set of neighbours of vertex i in G . The binary representation of these stabilisers is

$$S_{\text{graph}} = \begin{pmatrix} A \\ I_n \end{pmatrix}, \quad (10)$$

where A , an $n \times n$ symmetric matrix with 0s on its diagonal, is exactly the adjacency matrix of G .

It is well-known that $|\Phi_G\rangle = VH^{\otimes n}|0^n\rangle$ where V is a product of CZ gates and H is the HADAMARD gate. More specifically, V applies CZ between qubits i and j if and only if vertex i neighbours j in G . Van den Nest, Dehaene, and De Moor [40] tell us that *any* stabiliser state can be transformed to a graph state by a product of single-qubit Clifford gates. It is therefore clear that we can transform any S_{start} to S_{end} via S_{graph} using at most $n(n-1)/2$ two-qubit (CZ) gates, as this is the maximum number of edges on an n -vertex graph. The interesting question is whether we can do better by exploiting the potential low rank $k \leq n$ of S_{start} .

Our answer is in the affirmative and we now present an explicit and efficient algorithm that constructs U with at most $u_{cz}(k, n) = kn - k(k+1)/2$ two-qubit gates.

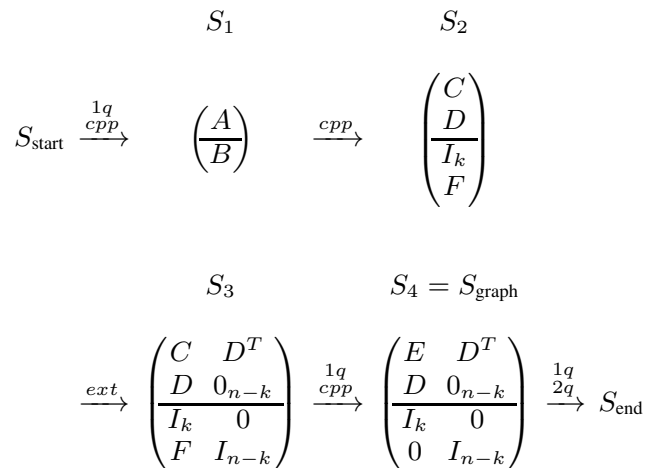


FIG. 1. Reductions used in our CZ-construction.

In Fig. 1, we illustrate the sequence of reductions that allow us to reach S_{graph} , and so S_{end} , from S_{start} . We now describe the salient aspects of each step:

- $S_{\text{start}} \rightarrow S_1$. Following [41, Lemma 6], we can apply HADAMARD gates so that B has rank k . By *cpp* row-swaps (relabelling of qubits), we can ensure that the first k rows of B have full-rank.
- $S_1 \rightarrow S_2$. Since the upper $k \times k$ submatrix of B has full-rank, *cpp* column operations can reduce it to I_k .
- $S_2 \rightarrow S_3$. We can directly verify that the extension to S_3 is valid by Eq. (7). Clearly S_3 has full column-rank n . The sparsity of our chosen extension shall play a crucial role in the reduced 2q-size of U when $k < n$ in both the CZ- and CNOT-constructions.
- $S_3 \rightarrow S_4 = S_{\text{graph}}$. Column operations can eliminate F , then PHASE gates can ensure E has zeros on its diagonal. Importantly, S_4 represents a graph state S_{graph} .
- $S_4 \rightarrow S_{\text{end}}$. HADAMARD and CZ gates can implement this final reduction as discussed above. The maximum number of CZ gates required to map S_4 to S_{end} equals the maximum number of off-diagonal 1s in the upper

half of S_4 . When $n = k$, this is $n(n-1)/2 = O(n^2)$. When $k \neq n$, this is $w_{cz}(k, n) = kn - k(k+1)/2$ due to sparsity of the upper half of S_4 which traces back to the *ext* step from $S_3 \rightarrow S_4$.

Note that in step $S_4 \rightarrow S_{\text{end}}$, we can first try to reduce the upper half of S_4 by single-qubit gates before applying CZ. One way to do this is to reduce the number of edges in the graph whose adjacency matrix is specified by the upper half of S_4 by the so-called ‘‘local complementation’’ operation [40, 48, 49]. This corresponds precisely to reducing the number of CZ gates in our CZ-construction.

B. CNOT-construction

$$\begin{array}{ccc}
 & S_5 & S_6 \\
 S_4 \xrightarrow[1q]{2q} \begin{pmatrix} 0_k & D^T \\ D & 0_{n-k} \\ M & 0 \\ 0 & I_{n-k} \end{pmatrix} \xrightarrow[cpp]{1q} & & \begin{pmatrix} I_k & D^T \\ D & I_{n-k} \\ I_k & 0 \\ 0 & I_{n-k} \end{pmatrix} \\
 \\
 & S_7 & S_8 \\
 \xrightarrow[2q]{1q} \begin{pmatrix} D_1 M_1 \\ M_1 \end{pmatrix} \xrightarrow[cpp]{1q} & & \begin{pmatrix} I_k - D^T D & 0 \\ 0 & I_{n-k} \\ I_k & 0 \\ 0 & I_{n-k} \end{pmatrix} \xrightarrow[2q]{1q} S_{\text{end}}
 \end{array}$$

FIG. 2. Reductions used in our CNOT-construction starting at S_4 of our CZ-construction.

We start from S_4 above which we reached without using two-qubit gates. Now, instead of using one block of CZ gates, we reduce to S_{end} as shown in Fig. 2, using three blocks of CNOT gates:

- $S_4 \rightarrow S_5$. Note that E must be symmetric by the commutativity condition given in Eq. (7). Then, following Ref. [41, Lemma 7], we can eliminate E using single-qubit and $O(k^2/\log k)$ CNOT gates. This is accomplished by noting that any symmetric binary E can be Cholesky decomposed as $E = \Lambda + M^T M$, with Λ diagonal and M invertible.
- $S_5 \rightarrow S_6$. Reduce M to I_k by column operations, then add 1s on the top diagonal by phase gates.
- $S_6 \rightarrow S_7$. Now, the upper $n \times n$ matrix can be block-Cholesky decomposed as

$$\begin{pmatrix} I_k & D^T \\ D & I_{n-k} \end{pmatrix} = M_1^T D_1 M_1, \quad (11)$$

where

$$M_1 := \begin{pmatrix} I_k & 0 \\ D & I_{n-k} \end{pmatrix}, \quad (12)$$

$$D_1 := \begin{pmatrix} I_k - D^T D & 0 \\ 0 & I_{n-k} \end{pmatrix}. \quad (13)$$

Next, we apply CNOT gates corresponding to M_1 . The number of CNOT gates required here equals the number of row operations required to reduce M_1 to I_n . We find this is at most $u_{cnot}(k, n) = O(kn/\log k)$ via arguments of Patel, Markov, and Hayes [42]. The proof is given in Appendix C.

- $S_7 \rightarrow S_8$. Multiply by M_1^{-1} on the right.
- $S_8 \rightarrow S_{\text{end}}$. $I_k - D^T D$ is a $k \times k$ symmetric matrix and so can be again eliminated via the Cholesky decomposition using $O(k^2/\log k)$ CNOT gates.

Note that in the three steps $S_4 \rightarrow S_5$, $S_6 \rightarrow S_7$, and $S_8 \rightarrow S_{\text{end}}$, we have used blocks of CNOT gates. The method we used to synthesise these blocks is size-optimal [42, Lemma 1], but we could have alternatively used methods in Ref. [50], that built on Ref. [51], to achieve optimal space-depth tradeoff, where space refers to extra ancilla qubits.

To end our discussion of constructing rotation circuits, we briefly mention a third, ancilla-based construction with $2q$ -size at most kn . This construction is well-known in the context of syndrome measurement [47] in quantum error correction but does not seem to have been mentioned in the context of measuring a Pauli decomposition of an observable, as in VQE. To measure k commuting Paulis $\{P_i\}_{i=1}^k$, this ‘‘ancilla-construction’’ uses k ancilla and involves k consecutive blocks of generalised-CNOT gates, each targeted at a different ancilla. The controls in block $b \leq k$ are activated or deactivated by the $+1$ or -1 eigenstates of the single-qubit Paulis forming P_b [52]. k single-qubit measurements are performed on the ancilla at the end of each block to exactly give measurements of P_i . Unfortunately, this construction requires k extra ancilla qubits and has worse worst-case $2q$ -size than both of our constructions. However, it does serve as a simple way to see, a priori, that a $2q$ -size scaling of $O(kn)$ is possible.

III. GROUPING STRATEGIES

Now that we have demonstrated the construction of a rotation circuit for a group of generally commuting Paulis, we would like to quantify the advantage offered, in terms of use of the quantum computer, in assembling operators into such groups. We have a Hamiltonian, H , of the form

$$H = \sum_{i=1}^N H_i = \sum_{i=1}^N \sum_{j=1}^{m_i} a_{ij} P_{ij} \quad (14)$$

where N is the number of groups of mutually commuting operators, m_i is the number of operators in group i , P_{ij} is the j th Pauli operator in the i th group and $a_{ij} \in \mathbb{R}$ is its coefficient.

Given ϵ , let M_u and M_g be the minimal number of measurements required to attain an accuracy ϵ in the ungrouped and grouped (as per Eq. 14) cases respectively. Finding M_u is a special case of finding M_g . To find M_g , we can solve the constrained optimisation problem that asks how a given number of measurements should be distributed in order to maximise accuracy. Following Ref. [8, 43, 44], we can use Lagrange multipliers to find

$$M_g = \left(\frac{1}{\epsilon} \sum_{i=1}^N \sqrt{\text{Var}[H_i]} \right)^2, \quad (15)$$

where

$$\text{Var}[H_i] = \langle H_i^2 \rangle - \langle H_i \rangle^2. \quad (16)$$

Since M_u is just M_g evaluated with every operator in its own group, we have

$$M_u = \left(\frac{1}{\epsilon} \sum_{i=1}^N \sum_{j=1}^{m_i} |a_{ij}| \sqrt{\text{Var}[P_{ij}]} \right)^2, \quad (17)$$

where

$$\text{Var}[P_{ij}] = 1 - \langle P_{ij} \rangle^2. \quad (18)$$

The ratio R , defined as

$$R := \frac{M_u}{M_g} = \left(\frac{\sum_{i=1}^N \sum_{j=1}^{m_i} |a_{ij}| \sqrt{\text{Var}[P_{ij}]} }{\sum_{i=1}^N \sqrt{\text{Var}[H_i]} } \right)^2, \quad (19)$$

therefore acts as a natural metric for the performance of a particular grouping under the assumption that measurements are distributed optimally. We prove as Claim 1 that combining two groups into one is always better with respect to R .

Claim 1. *Consider two groups \mathcal{C}_a and \mathcal{C}_b of mutually commuting Paulis, where each Pauli is in at most one group. Suppose that it is possible to combine \mathcal{C}_a and \mathcal{C}_b into a single commuting group, called $\mathcal{C}_{a \cup b}$. Let $R(\{\mathcal{C}_a, \mathcal{C}_b\})$ and $R(\{\mathcal{C}_{a \cup b}\})$ denote the R metric, as defined in Eq. (19), for the two groups separated and combined respectively. Then*

$$R(\{\mathcal{C}_a, \mathcal{C}_b\}) \geq R(\{\mathcal{C}_{a \cup b}\}). \quad (20)$$

Proof. As \sqrt{f} is a strictly increasing function for $f \in \mathbb{R}_{>0}$ and the numerator of R is independent of the grouping, it is sufficient to consider only the size of denominator of R

$$\sum_{i=1}^N \sqrt{\text{Var}[H_i]} \quad (21)$$

for the two cases. The variance of a single commuting group \mathcal{C}_i can be written as

$$\begin{aligned} \text{Var}[H_i] &= \text{Cov}[H_i, H_i] = \sum_{j,k} a_{ij}^* a_{ik} \text{Cov}[P_{ij}, P_{ik}] \\ &= \mathbf{a}_i^\dagger \mathbf{C} \mathbf{a}_i, \end{aligned} \quad (22)$$

where \mathbf{C} is the Hermitian and positive semi-definite covariance matrix for the state $|\psi\rangle$ and \mathbf{a}_i is a vector of the coefficients a_{ij} . \mathbf{C} is defined to have elements

$$C_{ij} := \text{Cov}[P_i, P_j] \quad \text{for all } P_i, P_j \in \mathcal{C}_i, \quad (23)$$

where the covariance $\text{Cov}[P_i, P_j]$ is defined as

$$\text{Cov}[P_i, P_j] := \langle P_i P_j \rangle_\psi - \langle P_i \rangle_\psi \langle P_j \rangle_\psi. \quad (24)$$

Let us now turn our attention to the single and two group comparison. We define coefficient vectors \mathbf{a} and \mathbf{b} , both of size $|\mathcal{C}_{a \cup b}|$, which contain the coefficients of the operators contained within groups \mathcal{C}_a and \mathcal{C}_b respectively. If a Pauli operator is not present within \mathcal{C}_a , the corresponding coefficient in \mathbf{a} will be zero, and similarly for \mathbf{b} and \mathcal{C}_b . The combined group $\mathcal{C}_{a \cup b}$ therefore has coefficients $\mathbf{a} + \mathbf{b}$. The contribution of the two separate groups to (22) is

$$\begin{aligned} & \sqrt{\mathbf{a}^\dagger \mathbf{C}_{ab} \mathbf{a}} + \sqrt{\mathbf{b}^\dagger \mathbf{C}_{ab} \mathbf{b}} \\ &= \sqrt{\left(\sqrt{\mathbf{a}^\dagger \mathbf{C}_{ab} \mathbf{a}} + \sqrt{\mathbf{b}^\dagger \mathbf{C}_{ab} \mathbf{b}} \right)^2} \\ &= \sqrt{\mathbf{a}^\dagger \mathbf{C}_{ab} \mathbf{a} + \mathbf{b}^\dagger \mathbf{C}_{ab} \mathbf{b} + 2\sqrt{(\mathbf{a}^\dagger \mathbf{C}_{ab} \mathbf{a})(\mathbf{b}^\dagger \mathbf{C}_{ab} \mathbf{b})}}, \end{aligned} \quad (25)$$

where \mathbf{C}_{ab} is the $|\mathcal{C}_{a \cup b}| \times |\mathcal{C}_{a \cup b}|$ covariance matrix of the full set of operators contained within $\mathcal{C}_{a \cup b}$. The contribution due to the single group is

$$\begin{aligned} & \sqrt{(\mathbf{a} + \mathbf{b})^\dagger \mathbf{C}_{ab} (\mathbf{a} + \mathbf{b})} \\ &= \sqrt{\mathbf{a}^\dagger \mathbf{C}_{ab} \mathbf{a} + \mathbf{b}^\dagger \mathbf{C}_{ab} \mathbf{b} + \mathbf{a}^\dagger \mathbf{C}_{ab} \mathbf{b} + \mathbf{b}^\dagger \mathbf{C}_{ab} \mathbf{a}} \\ &= \sqrt{\mathbf{a}^\dagger \mathbf{C}_{ab} \mathbf{a} + \mathbf{b}^\dagger \mathbf{C}_{ab} \mathbf{b} + 2\mathbf{a}^\dagger \mathbf{C}_{ab} \mathbf{b}}. \end{aligned} \quad (26)$$

Because \mathbf{C}_{ab} is positive semi-definite, we can define the semi-inner product $\langle \mathbf{a}, \mathbf{b} \rangle := \mathbf{a}^\dagger \mathbf{C}_{ab} \mathbf{b}$ [53, Example 1.1] and use the Cauchy-Schwarz inequality to find

$$(\mathbf{a}^\dagger \mathbf{C}_{ab} \mathbf{b})^2 \leq (\mathbf{a}^\dagger \mathbf{C}_{ab} \mathbf{a})(\mathbf{b}^\dagger \mathbf{C}_{ab} \mathbf{b}). \quad (27)$$

Equality holds if and only if there exist α and $\beta \in \mathbb{C}$, such that not both are equal to 0 and $\langle \alpha \mathbf{a} + \beta \mathbf{b}, \alpha \mathbf{a} + \beta \mathbf{b} \rangle = 0$ [53, Example 1.4]. Therefore, by comparison, (25) \geq (26) and so

$$R(\{\mathcal{C}_a, \mathcal{C}_b\}) \geq R(\{\mathcal{C}_{a \cup b}\}) \quad \text{for all } |\psi\rangle. \quad (28)$$

□

Claim 1 shows that it is impossible to mitigate covariances by splitting groups and using the optimal measurement strategy. This is in contrast to Refs. [3, 23], who showed that it is possible using a sub-optimal measurement strategy. In Appendix D, we re-do precisely their example using the optimal measurement strategy. Note that Claim 1 does not imply that the minimum number of groups is best, simply that it is never better to break a single group into two.

If all of the variances going into R are replaced by their expectation values over the uniform spherical measure (see Ref. [54, Ch. 7]), we obtain another metric, \hat{R} , given by

$$\hat{R} := \left(\frac{\sum_{i=1}^N \sum_{j=1}^{N_i} |a_{ij}|}{\sum_{i=1}^N \sqrt{\sum_{j=1}^{N_i} |a_{ij}|^2}} \right)^2. \quad (29)$$

The derivation of \hat{R} is given in Appendix E. The same proof as in Claim 1 can be used to show that breaking a group into two is never better when measured by \hat{R} ; the only difference is the covariance matrix must be replaced by its expectation over the uniform spherical measure.

\hat{R} is a particularly useful metric because it approximates $\mathbb{E}[R]$ over the uniform spherical measure, but can be calculated analytically. A good grouping strategy maximises \hat{R} by minimising the denominator. This is achieved by taking advantage of the concavity of the square root by placing the operators with the largest $|a_{ij}|^2$ coefficients in the same groups. Physically, this represents the optimal measurement scheme being able to direct many measurements towards a few groups with large variances. In the next paragraph, we propose a simple strategy for grouping operators motivated by this idea.

Given H , the strategy is to take each operator ordered by the absolute value of the coefficient, check if it can be placed in an existing group and, if not, start a new group. The groups are checked in order of creation. This is of complexity $nt(t-1)/2$ at worst, where we recall that n is the number of qubits and t is the number of Pauli terms in the Hamiltonian. We have named this strategy SORTED INSERTION.

Greedy colouring algorithms, as implemented in Ref. [19], require pre-generating the commutation graph which takes the same number of operations as the worst case scenario for SORTED INSERTION. The colouring algorithms then run on the graph adding their own complexity – see Table I. Therefore, SORTED INSERTION’s worst case complexity is bounded by the best case complexity of greedy colouring algorithms, such as those we will compare it to in Sec. IV.

Colouring Algorithm	Time Complexity
Largest First	$O(t^2)$
Connected Sequential d.f.s.	$O(t^2)$
DSATUR	$O(t^2 \log t)$
Independent Set	$O(t^3)$

TABLE I. Time complexities of the greedy colouring algorithms we compare with SORTED INSERTION in Sec. IV *after* pre-generating the commutation graph [55].

IV. APPLICATION TO VQE

In this section, we present numerical results of the grouping method discussed in Sec. III, alongside the CZ-construction of Sec. II A to construct the rotation circuits for given commuting groups. In particular, we have applied our methods

to the Hamiltonians of simple molecules so as to demonstrate their use in the context of VQE. The full results are given in Table IV, with a subset shown in Table II. In all cases, we used OpenFermion [57] to obtain Hamiltonians in the STO-3G basis, at approximately the equilibrium geometry of the molecules, with the symmetry conserving Bravyi-Kitaev transformation [17, 58]. In order to reduce the number of two-qubit gates required, we considered qubits on which all operators in a group locally commute separately – a one-qubit rotation per locally commuting qubit is all that is required to do so.

In Fig. 3(a), we plot the average group size against the number of qubits, n , for the molecular Hamiltonians. We can see that the average group size increases with increasing n , and the increase does not appear to be slowing down. We therefore conclude that our sorting method works well on systems of at least size $n = 38$. However, the key advantage of assembling a Hamiltonian into groups of mutually commuting operators is a reduction in the number of measurements required to obtain an energy expectation to a certain level of accuracy, and group size alone does not directly quantify this reduction. For a given Hamiltonian and quantum state, the reduction is instead given by R , as in Eq. (19).

We therefore calculated the value of R for 100 different quantum states, generated using 100 random sets of ansatz parameters with a hardware efficient ansatz of depth 1, for the nine smallest molecular systems. We show the mean, minimum and maximum values for each molecule. In practice, the value of R can at best be obtained approximately by making measurements on the quantum computer and so cannot be used to determine the expected advantage of a particular grouping a priori. The metric \hat{R} , given by Eq. (29), on the other hand, depends only on the coefficients of the terms in the Hamiltonian. From Table II, we can see that \hat{R} closely approximates the average of R over many ansatz parameters, but can be calculated analytically without the need for simulations. In Fig. 3(b), we show \hat{R} as a function of the number of qubits for our full selection of molecules. We can see that it is highly molecule dependent, with systems of similar size having very different values.

The reduction in number of measurements required comes at the cost of applying additional quantum gates before the qubits are measured, the most costly of which are two-qubit gates. For the CZ-construction, we demonstrated in Sec. II A that the maximum number of additional two-qubit gates required for a group with k independent terms is $nk - k(k+1)/2$. We would like to know, in practice, how many additional two-qubit gates are required at a maximum, as this is the quantum resource that is most limiting. Assuming for a given Hamiltonian that at least one group has rank n , obtaining a measurement of all terms in a Hamiltonian on n qubits may therefore require applying an additional $n(n-1)/2$ gates in a single circuit. However, for the molecules we have considered, we find that the largest number of two-qubit gates required is in fact far lower than this, typically by a factor of approximately 3.5, as can be seen in Fig. 3(c).

Given the close relationship between the average value of R and the value of \hat{R} , we propose using \hat{R} as a metric for the

Molecule	n qubits	t Paulis	Grouping			Ratios R, \hat{R}				Rotation Circuit $2q$ -size		
			N	$\overline{m_i}$	$\overline{k_i}$	R min	R mean	R max	\hat{R}	theory max	true max	mean
H ₂	2	4	2	2.00	1.50	1.09	1.93	4.60	1.76	0	0	0
H ₃ ⁺	4	59	10	5.90	3.50	3.76	11.92	33.04	10.25	6	3	0.80
LiH	10	630	41	15.37	6.85	19.60	24.91	34.74	23.97	45	18	5.29
OH ⁻	10	630	38	16.58	7.29	6.32	8.90	12.86	8.51	45	17	5.63
HF	10	630	39	16.15	6.97	6.07	8.57	12.27	8.21	45	16	5.74
H ₂ O	12	1085	51	21.27	9.04	7.68	11.27	16.96	10.67	66	26	7.37
BH ₃	14	1584	66	24.00	10.36	17.21	20.93	32.13	20.05	91	26	9.56
NH ₃	14	3608	118	30.58	11.34	12.65	15.96	26.93	15.31	91	28	10.26
CH ₄	16	3887	123	31.60	13.39	16.96	21.63	29.33	20.27	120	45	16.75

TABLE II. A reduced set of results of the numerical simulations discussed in the main text, and shown in full in Table IV. For each molecule, we show a number of results related to the grouping of Hamiltonian terms, how the grouping reduces the number of measurements required using the metrics R and \hat{R} , and the number of two-qubit gates in the resulting rotation circuits. Note that the mean value of R and \hat{R} are very similar.

Molecule	Largest First		Connected Sequential d.f.s.		Independent Set		DSATUR		SORTED INSERTION	
	N	\hat{R}	N	\hat{R}	N	\hat{R}	N	\hat{R}	N	\hat{R}
H ₂	2	1.76	2	1.76	2	1.76	2	1.76	2	1.76
H ₃ ⁺	10	4.86	10	10.25	10	10.30	9	4.10	10	10.25
LiH	39	23.87	45	23.33	30	5.72	29	10.47	41	23.97
OH ⁻	40	8.27	41	8.41	21	3.00	28	3.23	37	8.51
HF	38	8.05	41	8.07	21	2.80	28	3.23	38	8.21
H ₂ O	57	2.98	55	10.66	42	3.87	51	3.18	51	10.66
BH ₃	66	4.80	85	18.70	60	7.85	72	4.11	68	20.05
NH ₃	124	6.50	174	13.97	126	4.03	137	2.92	117	15.31
CH ₄	122	5.84	176	18.93	114	9.88	110	4.90	125	20.27
O ₂	62	13.62	85	19.95	42	6.79	52	7.91	67	20.23
N ₂	62	15.00	86	21.15	39	8.37	49	5.80	78	22.10
CO	124	20.70	155	20.67	89	6.03	106	4.55	128	21.31
HCl	117	2.16	141	10.29	98	3.52	104	2.04	123	10.36
NaH	121	8.78	181	12.40	149	3.44	145	3.65	135	12.90
H ₂ S	122	8.81	180	12.45	147	3.80	145	3.66	147	11.60

TABLE III. Comparison of the groupings produced by the greedy colouring algorithms “Largest First”, “Connected Sequential d.f.s.” (depth first search), “Independent Set” and “DSATUR” as implemented by the Python package NetworkX [56] with our method SORTED INSERTION. For each method, the number of groups produced, N , and the metric \hat{R} given by equation (29), are presented. The best or joint best methods are highlighted in bold for each molecule.

quality of a grouping method and compare different methods of grouping the operators with this metric in mind. The results are shown in Table III, along with the number of groups of operators, N , that each method produces. Out of the methods, “Independent Set” was best at approximating the minimum clique cover – it found the cover with the fewest cliques in all but one case. However, it appears that the minimum clique cover does not necessarily result in the fewest measurements, with “Independent Set” only performing best once with re-

spect to \hat{R} . Overall, our SORTED INSERTION was best at maximising \hat{R} , performing best or joint best in all but two cases.

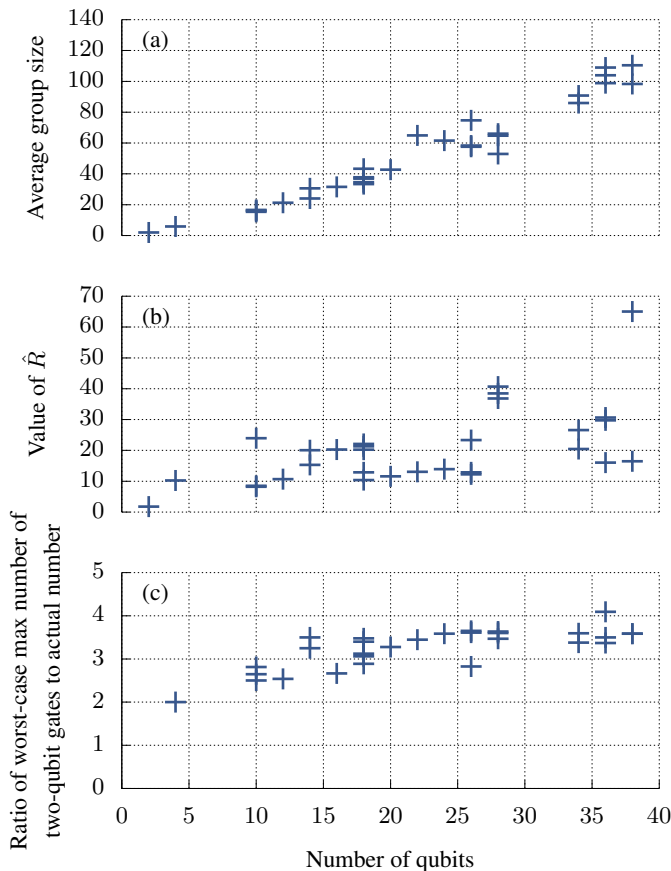


FIG. 3. The results of numerical simulations discussed in the text. We show (a) the average group size, (b) the value of \hat{R} , given by Eq. (29), and (c) the ratio of the worst-case maximum number of two-qubit gates in a single rotation circuit to the actual number as a function of the number of qubits for a range of simple molecules. A subset of the data is shown in Table II, and the full data is shown in Table IV.

V. CONCLUSION

We have addressed two problems related to the efficient measurement of Pauli operators on a quantum computer. The first is how to synthesise rotation circuits that enable mutually commuting Paulis to be measured simultaneously, and the second is how to assemble a set of Paulis into groups in which they mutually commute.

We have contributed two rotation circuit constructions CZ and CNOT. The CZ-construction results in a maximum of $u_{cz}(k, n) = kn - k(k + 1)/2$ two-qubit gates while the CNOT-construction results in a maximum of $u_{cnot}(k, n) = O(kn/\log k)$. On grouping Pauli operators, we contribute two natural metrics, R and \hat{R} , that justifiably measure the effectiveness of a grouping. We also contribute a grouping strategy motivated by \hat{R} that we call SORTED INSERTION.

We have applied our theoretical work to the task of estimating energies of molecules in the context of VQE. We find that, for the CZ-construction, the largest number of two-qubit gates required is typically less than the theoretical worst-case by a factor of approximately 3.5. Comparison to other grouping methods shows that while SORTED INSERTION does not normally result in the smallest number of groups, it nearly always results in the best value of \hat{R} .

VI. ACKNOWLEDGEMENT

We thank Oscar Higgott for informing us of the ancilla-based simultaneous measurement method and Ref. [59, Fig. 14].

-
- [1] Alberto Peruzzo, Jarrod McClean, Peter Shadbolt, Man-Hong Yung, Xiao-Qi Zhou, Peter J Love, Alán Aspuru-Guzik, and Jeremy L OBrien, “A variational eigenvalue solver on a photonic quantum processor,” *Nature communications* **5**, 4213 (2014).
- [2] John Preskill, “Quantum computing in the NISQ era and beyond,” *Quantum* **2**, 79 (2018).
- [3] Jarrod R McClean, Jonathan Romero, Ryan Babbush, and Alán Aspuru-Guzik, “The theory of variational hybrid quantum-classical algorithms,” *New Journal of Physics* **18**, 023023 (2016).
- [4] P. J. J. O’Malley, R. Babbush, I. D. Kivlichan, J. Romero, J. R. McClean, R. Barends, J. Kelly, P. Roushan, A. Tranter, N. Ding, B. Campbell, P. J. Love, H. Neven, A. Aspuru-Guzik, J. M. Martinis, *et al.*, “Scalable quantum simulation of molecular energies,” *Phys. Rev. X* **6**, 031007 (2016).
- [5] Abhinav Kandala, Antonio Mezzacapo, Kristan Temme, Maika Takita, Markus Brink, Jerry M. Chow, and Jay M. Gambetta, “Hardware-efficient variational quantum eigensolver for small molecules and quantum magnets,” *Nature* **549**, 242 EP – (2017).
- [6] Sam McArdle, Suguru Endo, Alan Aspuru-Guzik, Simon Benjamin, and Xiao Yuan, “Quantum computational chemistry,” *arXiv e-prints* (2018), arXiv:1808.10402 [quant-ph].
- [7] Ilya G. Ryabinkin, Scott N. Genin, and Artur F. Izmaylov, “Constrained variational quantum eigensolver: Quantum computer search engine in the fock space,” *Journal of Chemical Theory and Computation, Journal of Chemical Theory and Computation* **15**, 249–255 (2019).
- [8] Jonathan Romero, Ryan Babbush, Jarrod R McClean, Cornelius Hempel, Peter J Love, and Alán Aspuru-Guzik, “Strategies for quantum computing molecular energies using the unitary coupled cluster ansatz,” *Quantum Science and Technology* **4**, 014008 (2018).
- [9] Daochen Wang, Oscar Higgott, and Stephen Brerley, “Accelerated variational quantum eigensolver,” *Phys. Rev. Lett.* **122**, 140504 (2019).
- [10] Jarrod R McClean, Mollie E Kimchi-Schwartz, Jonathan Carter, and Wibe A de Jong, “Hybrid quantum-classical hierarchy for mitigation of decoherence and determination of excited

- states,” *Physical Review A* **95**, 042308 (2017).
- [11] Raffaele Santagati, Jianwei Wang, Antonio A. Gentile, Stefano Paesani, Nathan Wiebe, Jarrod R. McClean, Sam Morley-Short, Peter J. Shadbolt, Damien Bonneau, Joshua W. Silverstone, David P. Tew, Xiaoqi Zhou, Jeremy L. O’Brien, and Mark G. Thompson, “Witnessing eigenstates for quantum simulation of hamiltonian spectra,” *Science Advances* **4** (2018), 10.1126/sciadv.aap9646.
- [12] J. I. Colless, V. V. Ramasesh, D. Dahlen, M. S. Blok, M. E. Kimchi-Schwartz, J. R. McClean, J. Carter, W. A. de Jong, and I. Siddiqi, “Computation of molecular spectra on a quantum processor with an error-resilient algorithm,” *Phys. Rev. X* **8**, 011021 (2018).
- [13] Kentaro Heya, Ken M Nakanishi, Kosuke Mitarai, and Keisuke Fujii, “Subspace Variational Quantum Simulator,” arXiv e-prints (2019), arXiv:1904.08566 [quant-ph].
- [14] Tyson Jones, Suguru Endo, Sam McArdle, Xiao Yuan, and Simon C. Benjamin, “Variational quantum algorithms for discovering Hamiltonian spectra,” *Phys. Rev. A* **99**, 062304 (2019).
- [15] Oscar Higgott, Daochen Wang, and Stephen Brierley, “Variational Quantum Computation of Excited States,” *Quantum* **3**, 156 (2019).
- [16] P. Jordan and E. Wigner, “Über das paulische äquivalenzverbot,” *Zeitschrift für Physik* **47**, 631–651 (1928).
- [17] Sergey Bravyi, Jay M. Gambetta, Antonio Mezzacapo, and Kristan Temme, “Tapering off qubits to simulate fermionic Hamiltonians,” arXiv e-prints (2017), arXiv:1701.08213 [quant-ph].
- [18] F Verstraete and J I Cirac, “Mapping local Hamiltonians of fermions to local Hamiltonians of spins,” *Journal of Statistical Mechanics: Theory and Experiment* **2005** (2005).
- [19] Vladyslav Verteletskyi, Tzu-Ching Yen, and Artur F. Izmaylov, “Measurement Optimization in the Variational Quantum Eigensolver Using a Minimum Clique Cover,” arXiv e-prints (2019), arXiv:1907.03358 [quant-ph].
- [20] Andrew Jena, Scott Genin, and Michele Mosca, “Pauli Partitioning with Respect to Gate Sets,” arXiv e-prints (2019), arXiv:1907.07859 [quant-ph].
- [21] Tzu-Ching Yen, Vladyslav Verteletskyi, and Artur F. Izmaylov, “Measuring all compatible operators in one series of a single-qubit measurements using unitary transformations,” arXiv e-prints (2019), arXiv:1907.09386 [quant-ph].
- [22] William J. Huggins, Jarrod McClean, Nicholas Rubin, Zhang Jiang, Nathan Wiebe, K. Birgitta Whaley, and Ryan Babush, “Efficient and Noise Resilient Measurements for Quantum Chemistry on Near-Term Quantum Computers,” arXiv e-prints (2019), arXiv:1907.13117 [quant-ph].
- [23] Pranav Gokhale, Olivia Angiuli, Yongshan Ding, Kaiwen Gui, Teague Tomesh, Martin Suchara, Margaret Martonosi, and Frederic T. Chong, “Minimizing State Preparations in Variational Quantum Eigensolver by Partitioning into Commuting Families,” arXiv e-prints (2019), arXiv:1907.13623 [quant-ph].
- [24] We mention that both the grouping and rotation construction problems have been addressed on an ad-hoc basis by experimentalists since Kandala *et al.* [60]. We refer readers to Table 2 of Ref. [23] for a good summary. We also mention that recent Ref. [61] and the less recent Ref. [62] allow for grouping of non-commuting Paulis. We found it interesting that such approaches are feasible, but found it hard to compare them to our work on a like-for-like basis.
- [25] Alexandre Blais, Jay Gambetta, A. Wallraff, D. I. Schuster, S. M. Girvin, M. H. Devoret, and R. J. Schoelkopf, “Quantum-information processing with circuit quantum electrodynamics,” *Phys. Rev. A* **75**, 032329 (2007).
- [26] Anthony Laing, Alberto Peruzzo, Alberto Politi, Maria Rodas Verde, Matthaeus Halder, Timothy C. Ralph, Mark G. Thompson, and Jeremy L. O’Brien, “High-fidelity operation of quantum photonic circuits,” *Applied Physics Letters* **97**, 211109 (2010), <https://doi.org/10.1063/1.3497087>.
- [27] R. Barends, J. Kelly, A. Megrant, A. Veitia, D. Sank, E. Jeffrey, T. C. White, J. Mutus, A. G. Fowler, B. Campbell, Y. Chen, Z. Chen, B. Chiaro, A. Dunsworth, C. Neill, P. O’Malley, P. Roushan, A. Vainsencher, J. Wenner, A. N. Korotkov, A. N. Cleland, and John M. Martinis, “Superconducting quantum circuits at the surface code threshold for fault tolerance,” *Nature* **508**, 500 EP – (2014).
- [28] C. J. Ballance, T. P. Harty, N. M. Linke, M. A. Sepiol, and D. M. Lucas, “High-fidelity quantum logic gates using trapped-ion hyperfine qubits,” *Phys. Rev. Lett.* **117**, 060504 (2016).
- [29] Joseph L. Allen, Robert Kosut, Jaewoo Joo, Peter Leek, and Eran Ginossar, “Optimal control of two qubits via a single cavity drive in circuit quantum electrodynamics,” *Phys. Rev. A* **95**, 042325 (2017).
- [30] Norbert M. Linke, Dmitri Maslov, Martin Roetteler, Shantanu Debnath, Caroline Figgatt, Kevin A. Landsman, Kenneth Wright, and Christopher Monroe, “Experimental comparison of two quantum computing architectures,” *Proceedings of the National Academy of Sciences* **114**, 3305–3310 (2017), <https://www.pnas.org/content/114/13/3305.full.pdf>.
- [31] G Wendin, “Quantum information processing with superconducting circuits: a review,” *Reports on Progress in Physics* **80**, 106001 (2017).
- [32] Matthew Reagor, Christopher B. Osborn, Nikolas Tezak, Alexa Staley, Guenevere Prawiroatmodjo, Michael Scheer, Nasser Alidoust, Eyob A. Sete, Nicolas Didier, Marcus P. da Silva, Ezer Acala, Joel Angeles, Andrew Bestwick, Maxwell Block, Chad T. Rigetti, *et al.*, “Demonstration of universal parametric entangling gates on a multi-qubit lattice,” *Science Advances* **4** (2018), 10.1126/sciadv.aao3603, <https://advances.sciencemag.org/content/4/2/eaao3603.full.pdf>.
- [33] V. M. Schäfer, C. J. Ballance, K. Thirumalai, L. J. Stephenson, T. G. Ballance, A. M. Steane, and D. M. Lucas, “Fast quantum logic gates with trapped-ion qubits,” *Nature* **555**, 75 EP – (2018).
- [34] A. E. Webb, S. C. Webster, S. Collingbourne, D. Braud, A. M. Lawrence, S. Weidt, F. Mintert, and W. K. Hensinger, “Resilient entangling gates for trapped ions,” *Phys. Rev. Lett.* **121**, 180501 (2018).
- [35] Harry Levine, Alexander Keesling, Ahmed Omran, Hannes Bernien, Sylvain Schwartz, Alexander S. Zibrov, Manuel Endres, Markus Greiner, Vladan Vuletić, and Mikhail D. Lukin, “High-fidelity control and entanglement of Rydberg-atom qubits,” *Phys. Rev. Lett.* **121**, 123603 (2018).
- [36] Y. He, S. K. Gorman, D. Keith, L. Kranz, J. G. Keizer, and M. Y. Simmons, “A two-qubit gate between phosphorus donor electrons in silicon,” *Nature* **571**, 371–375 (2019).
- [37] W. Huang, C. H. Yang, K. W. Chan, T. Tanttu, B. Hensen, R. C. C. Leon, M. A. Fogarty, J. C. C. Hwang, F. E. Hudson, K. M. Itoh, A. Morello, A. Laucht, and A. S. Dzurak, “Fidelity benchmarks for two-qubit gates in silicon,” *Nature* **569**, 532–536 (2019).
- [38] Reinhold Blumel, Nikodem Grzesiak, and Yunseong Nam, “Power-optimal, stabilized entangling gate between trapped-ion qubits,” arXiv e-prints (2019), arXiv:1905.09292 [quant-ph].
- [39] Y. He, S. K. Gorman, D. Keith, L. Kranz, J. G. Keizer, and M. Y. Simmons, “A two-qubit gate between phosphorus donor

- electrons in silicon,” *Nature* **571**, 371–375 (2019).
- [40] Maarten Van den Nest, Jeroen Dehaene, and Bart De Moor, “Graphical description of the action of local Clifford transformations on graph states,” *Phys. Rev. A* **69**, 022316 (2004).
- [41] Scott Aaronson and Daniel Gottesman, “Improved simulation of stabilizer circuits,” *Phys. Rev. A* **70**, 052328 (2004).
- [42] Ketan N. Patel, Igor L. Markov, and John P. Hayes, “Optimal synthesis of linear reversible circuits,” *Quantum Info. Comput.* **8**, 282–294 (2008).
- [43] Dave Wecker, Matthew B. Hastings, and Matthias Troyer, “Progress towards practical quantum variational algorithms,” *Phys. Rev. A* **92**, 042303 (2015).
- [44] Nicholas C Rubin, Ryan Babbush, and Jarrod McClean, “Application of fermionic marginal constraints to hybrid quantum algorithms,” *New Journal of Physics* **20**, 053020 (2018).
- [45] A. R. Calderbank, E. M. Rains, P. W. Shor, and N. J. A. Sloane, “Quantum error correction and orthogonal geometry,” *Phys. Rev. Lett.* **78**, 405–408 (1997).
- [46] Daniel Gottesman, *Stabilizer codes and quantum error correction*, Ph.D. thesis, California Institute of Technology (1997).
- [47] Michael A. Nielsen and Isaac L. Chuang, *Quantum Computation and Quantum Information: 10th Anniversary Edition*, 10th ed. (Cambridge University Press, New York, NY, USA, 2011).
- [48] M. Hein, J. Eisert, and H. J. Briegel, “Multiparty entanglement in graph states,” *Phys. Rev. A* **69**, 062311 (2004).
- [49] Andr Bouchet, “Recognizing locally equivalent graphs,” *Discrete Mathematics* **114**, 75 – 86 (1993).
- [50] Jiaqing Jiang, Xiaoming Sun, Shang-Hua Teng, Bujiao Wu, Kewen Wu, and Jialin Zhang, “Optimal Space-Depth Trade-Off of CNOT Circuits in Quantum Logic Synthesis,” arXiv e-prints (2019), arXiv:1907.05087 [quant-ph].
- [51] Christopher Moore and Martin Nilsson, “Parallel Quantum Computation and Quantum Codes,” arXiv e-prints (1998), arXiv:quant-ph/9808027 [quant-ph].
- [52] So Z corresponds to standard control on $\{|0\rangle, |1\rangle\}$, X corresponds to control on $\{|+\rangle, |-\rangle\}$, Y corresponds to control on $\{|+i\rangle, |-i\rangle\}$, and I corresponds to not having a generalised-CNOT. These generalised-CNOT gates can be implemented by the standard CNOT conjugated by H in case of X , or SH in case of Y .
- [53] J.B. Conway, *A Course in Functional Analysis*, Graduate Texts in Mathematics (Springer New York, 1994).
- [54] John Watrous, *The Theory of Quantum Information* (Cambridge University Press, 2018).
- [55] Adrian Kosowski and Krzysztof Manuszewski, “Classical coloring of graphs,” (2004).
- [56] Aric A. Hagberg, Daniel A. Schult, and Pieter J. Swart, “Exploring network structure, dynamics, and function using NetworkX,” in *Proceedings of the 7th Python in Science Conference*, edited by Gal Varoquaux, Travis Vaught, and Jarrod Millman (2008) pp. 11 – 15.
- [57] Jarrod R. McClean, Kevin J. Sung, Ian D. Kivlichan, Yudong Cao, Chengyu Dai, E. Schuyler Fried, Craig Gidney, Brendan Gimby, Pranav Gokhale, Thomas Häner, Tarini Hardikar, Vojtěch Havlíček, Oscar Higgott, Cupjin Huang, Ryan Babbush, *et al.*, “OpenFermion: The Electronic Structure Package for Quantum Computers,” arXiv e-prints (2017), arXiv:1710.07629 [quant-ph].
- [58] Sergey B. Bravyi and Alexei Yu. Kitaev, “Fermionic Quantum Computation,” *Annals of Physics* **298**, 210–226 (2002), arXiv:quant-ph/0003137 [quant-ph].
- [59] Eric Dennis, Alexei Kitaev, Andrew Landahl, and John Preskill, “Topological quantum memory,” *Journal of Mathematical Physics* **43**, 4452–4505 (2002), arXiv:quant-ph/0110143 [quant-ph].
- [60] Abhinav Kandala, Antonio Mezzacapo, Kristan Temme, Maika Takita, Markus Brink, Jerry M. Chow, and Jay M. Gambetta, “Hardware-efficient variational quantum eigensolver for small molecules and quantum magnets,” *Nature* **549**, 242 EP – (2017).
- [61] Artur F. Izmaylov, Tzu-Ching Yen, Robert A. Lang, and Vladyslav Verteletskyi, “Unitary partitioning approach to the measurement problem in the Variational Quantum Eigensolver method,” arXiv e-prints (2019), arXiv:1907.09040 [quant-ph].
- [62] Artur F. Izmaylov, Tzu-Ching Yen, and Ilya G. Ryabinkin, “Revising the measurement process in the variational quantum eigensolver: is it possible to reduce the number of separately measured operators?” *Chem. Sci.* **10**, 3746–3755 (2019).
- [63] V.L. Arlazarov, E.A. Dinic, M.A. Kronod, and I.A. Faradez, “On economical construction of the transitive closure of an oriented graph,” *Soviet Mathematics Doklady*, 1209–10 (1970).
- [64] Robert M. Parrish, Lori A. Burns, Daniel G. A. Smith, Andrew C. Simmonett, A. Eugene DePrince, Edward G. Hohenstein, Uur Bozkaya, Alexander Yu. Sokolov, Roberto Di Remigio, Ryan M. Richard, Jrme F. Gonthier, Andrew M. James, Harley R. McAlexander, Ashutosh Kumar, C. David Sherrill, *et al.*, “Psi4 1.1: An open-source electronic structure program emphasizing automation, advanced libraries, and interoperability,” *Journal of Chemical Theory and Computation*, *Journal of Chemical Theory and Computation* **13**, 3185–3197 (2017).

Appendix A: Binary representation

The Pauli group \mathcal{P}_n on n -qubits is a group of 4^{n+1} elements defined by

$$\mathcal{P}_n = \{i^k \sigma_1 \otimes \cdots \otimes \sigma_n \mid \sigma_i \in \{I, X, Y, Z\}, k \in \{0, 1, 2, 3\}\} \quad (\text{A1})$$

The binary representation, first introduced by Calderbank, Rains, Shor, and Sloane [45], is a representation of \mathcal{P}_n as binary vectors. In this representation, Paulis differing only in phase i^k are represented in the same way.

Single-qubit Paulis are represented by 2-dimensional binary vectors, so that

$$\begin{aligned} \sigma_{00} &:= I \mapsto (0, 0), \\ \sigma_{01} &:= X \mapsto (0, 1), \\ \sigma_{10} &:= Z \mapsto (1, 0), \\ \sigma_{11} &:= Y \mapsto (1, 1). \end{aligned} \quad (\text{A2})$$

An n -qubit Pauli

$$\sigma_{u_1 v_1} \otimes \cdots \otimes \sigma_{u_n v_n} \quad (\text{A3})$$

is then represented by the $2n$ -dimensional binary vector

$$(u_1, \dots, u_n, v_1, \dots, v_n). \quad (\text{A4})$$

In this representation, two n -qubit Paulis with binary vectors a and b commute if and only if

$$a^T J_{2n} b = 0, \quad (\text{A5})$$

where J_{2n} denotes the $2n \times 2n$ matrix

$$J_{2n} := \begin{pmatrix} 0 & I_n \\ I_n & 0 \end{pmatrix}. \quad (\text{A6})$$

Given a set \mathcal{S} of m n -qubit Paulis, we can write down a corresponding $2n \times m$ binary matrix S where each column represents a Pauli. Then, from Eq. (A5), we deduce that all Paulis in \mathcal{S} mutually commute if and only if

$$S^T J_{2n} S = 0_m, \quad (\text{A7})$$

which recovers Eq. (7) in the main text. We say that the set \mathcal{S} of Paulis is independent if the matrix S has rank m .

We shall often find it helpful to write S in terms of its upper half $S^{(Z)}$ and lower half $S^{(X)}$, separated by a horizontal line for visual-aid, i.e.,

$$S = \begin{pmatrix} S^{(Z)} \\ S^{(X)} \end{pmatrix}. \quad (\text{A8})$$

The conjugation action of quantum gates on \mathcal{S} can be represented as transformations to the matrix S . For example, we document the transformations on \mathcal{S} that represent four common quantum gates. In the following, addition is mod 2 and p ranges over all columns $\{1, \dots, m\}$.

- CZ on qubits i and j :

$$\begin{aligned} S_{ip} &\leftarrow S_{ip} + S_{j+n,p}, \\ S_{jp} &\leftarrow S_{jp} + S_{i+n,p}. \end{aligned}$$
- CNOT on control-qubit i and target-qubit j :

$$\begin{aligned} S_{ip} &\leftarrow S_{ip} + S_{jp}, \\ S_{j+n,p} &\leftarrow S_{j+n,p} + S_{i+n,p}. \end{aligned}$$
- HADAMARD (H) on qubit i :

$$S_{ip} \leftrightarrow S_{i+n,p}.$$
- PHASE (P) on qubit i :

$$S_{ip} \leftarrow S_{ip} + S_{i+n,p}.$$

These rules can be directly verified by conjugating X_i, X_j, Z_i, Z_j by the listed gates. They are also reproduced in Sec. II of the main text.

Appendix B: CZ-construction example

We walk through our CZ-construction for a specific example. In this example, we would like to obtain measurements simultaneously of a set $\mathcal{S}'_{\text{start}}$ of six four-qubit Paulis given by

$$\begin{aligned} P_1 &= Z_1 Z_2 Z_3 Z_4, \\ P_2 &= X_1 X_2 Y_3 Y_4, \\ P_3 &= Y_1 Y_2 X_3 X_4, \\ P_4 &= Y_2 X_3, \\ P_5 &= Y_1 X_4, \\ P_6 &= X_1 Z_2 Z_3 Y_4. \end{aligned} \quad (\text{B1})$$

We can represent these Paulis in a matrix $\mathcal{S}'_{\text{start}}$ with

$$\mathcal{S}'_{\text{start}} = \begin{pmatrix} 1 & 0 & 1 & 0 & 1 & 0 \\ 1 & 0 & 1 & 1 & 0 & 1 \\ 1 & 1 & 0 & 0 & 0 & 1 \\ 1 & 1 & 0 & 0 & 0 & 1 \\ 0 & 1 & 1 & 0 & 1 & 1 \\ 0 & 1 & 1 & 1 & 0 & 0 \\ 0 & 1 & 1 & 1 & 0 & 0 \\ 0 & 1 & 1 & 0 & 1 & 1 \end{pmatrix}. \quad (\text{B2})$$

By Gaussian elimination, we find the reduced row echelon form of $\mathcal{S}'_{\text{start}}$ to be

$$\begin{pmatrix} 1 & 0 & 1 & 0 & 1 & 0 \\ 0 & 1 & 1 & 0 & 1 & 1 \\ 0 & 0 & 0 & 1 & 1 & 1 \\ 0 & 0 & 0 & 0 & 0 & 0 \\ \hline 0 & 0 & 0 & 0 & 0 & 0 \\ 0 & 0 & 0 & 0 & 0 & 0 \\ 0 & 0 & 0 & 0 & 0 & 0 \\ 0 & 0 & 0 & 0 & 0 & 0 \end{pmatrix}. \quad (\text{B3})$$

The pivot columns are numbers 1, 2 and 4 which tells us that P_1, P_2 and P_4 are the three independent Paulis from which

the remaining Paulis in S'_{start} can be constructed. Therefore, we can write $S'_{\text{start}} = S_{\text{start}}R_0^{-1}$, where

$$S_{\text{start}} := \begin{pmatrix} 1 & 0 & 0 \\ 1 & 0 & 1 \\ 1 & 1 & 0 \\ 1 & 1 & 0 \\ 0 & 1 & 0 \\ 0 & 1 & 1 \\ 0 & 1 & 1 \\ 0 & 1 & 0 \end{pmatrix}, R_0^{-1} := \begin{pmatrix} 1 & 0 & 1 & 0 & 1 & 0 \\ 0 & 1 & 1 & 0 & 1 & 1 \\ 0 & 0 & 0 & 1 & 1 & 1 \end{pmatrix}. \quad (\text{B4})$$

Note that the inverse on R_0^{-1} is purely notational. Now, the lower half $S_{\text{start}}^{(X)}$ of S_{start} has column echelon form

$$S_{\text{start}}^{(X)} = \begin{pmatrix} 1 & 0 & 0 \\ 1 & 1 & 0 \\ 1 & 1 & 0 \\ 1 & 0 & 0 \end{pmatrix}, \quad (\text{B5})$$

and so the first two rows are pivot rows. In order to give the lower half of S_{start} a rank of $k = 3$, we therefore apply a HADAMARD to the rows corresponding to qubits 3 and 4 so that

$$S_1 := Q_1 S_{\text{start}} = \begin{pmatrix} 1 & 0 & 0 \\ 1 & 0 & 1 \\ 0 & 1 & 1 \\ 0 & 1 & 0 \\ 0 & 1 & 0 \\ 0 & 1 & 1 \\ 1 & 1 & 0 \\ 1 & 1 & 0 \end{pmatrix} \quad (\text{B6})$$

where

$$Q_1 := \left(\begin{array}{ccc|ccc} 1 & 0 & 0 & 0 & 0 & 0 & 0 \\ 0 & 1 & 0 & 0 & 0 & 0 & 0 \\ 0 & 0 & 0 & 0 & 0 & 1 & 0 \\ 0 & 0 & 0 & 0 & 0 & 0 & 1 \\ \hline 0 & 0 & 0 & 0 & 1 & 0 & 0 & 0 \\ 0 & 0 & 0 & 0 & 0 & 1 & 0 & 0 \\ 0 & 0 & 1 & 0 & 0 & 0 & 0 & 0 \\ 0 & 0 & 0 & 1 & 0 & 0 & 0 & 0 \end{array} \right). \quad (\text{B7})$$

The lower half of S_1 now has rank 3, and performing Gaussian elimination on it, we find

$$S_2 := Q_1 S_{\text{start}} R_1 = \begin{pmatrix} 1 & 0 & 1 \\ 0 & 1 & 1 \\ 0 & 1 & 0 \\ 1 & 0 & 0 \\ 1 & 0 & 0 \\ 0 & 1 & 0 \\ 0 & 0 & 1 \\ 0 & 0 & 1 \end{pmatrix}, \quad (\text{B8})$$

where

$$R_1 = \begin{pmatrix} 0 & 1 & 0 \\ 0 & 1 & 1 \\ 1 & 1 & 0 \end{pmatrix}^{-1} = \begin{pmatrix} 1 & 0 & 1 \\ 1 & 0 & 0 \\ 1 & 1 & 0 \end{pmatrix}. \quad (\text{B9})$$

We now extend S_2 to a rank $n = 4$ matrix by adding a column that corresponds to a fourth Pauli P_{ext} . In the main text, this is the crucial *ext* step from $S_2 \rightarrow S_3$ which might have seemed fortuitous. In fact, *ext* was systematically obtained as follows.

To make our reasoning clearer, let us represent S_2 alternatively by the matrix

$$P(S_2) := \begin{pmatrix} Y & I & I & Z \\ I & Y & Z & I \\ Z & Z & X & X \end{pmatrix}, \quad (\text{B10})$$

where each row corresponds to a Pauli operator given by a column of S_2 . Looking at the form of $P(S_2)$, we see that we can place X in the 4th qubit position of P_{ext} (and nowhere else) to ensure P_{ext} is independent of the other Paulis. Then we observe that the left 3-by-3 sub-matrix of $P(S_2)$ has X/Y on the diagonal and I/Z everywhere else. This means we can place I/Z in the other qubit positions of P_{ext} depending on whether the X in its 4th qubit position commutes with the 4th position terms of the other Paulis.

By this prescription, we find $P_{\text{ext}} = Z_1 I_2 I_3 X_4$. Therefore S_2 is extended to

$$S_3 := \begin{pmatrix} 1 & 0 & 1 & 1 \\ 0 & 1 & 1 & 0 \\ 0 & 1 & 0 & 0 \\ 1 & 0 & 0 & 0 \\ \hline 1 & 0 & 0 & 0 \\ 0 & 1 & 0 & 0 \\ 0 & 0 & 1 & 0 \\ 0 & 0 & 1 & 1 \end{pmatrix}. \quad (\text{B11})$$

and

$$Q_1 S_{\text{start}} R_1 = S_3 R_2^{-1}, \quad (\text{B12})$$

where

$$R_2^{-1} := \begin{pmatrix} 1 & 0 & 0 \\ 0 & 1 & 0 \\ 0 & 0 & 1 \\ 0 & 0 & 0 \end{pmatrix} \quad (\text{B13})$$

Note that the inverse on R_2^{-1} is also purely notational. The lower half of S_3 is full-rank and so we can take its inverse to find

$$R_3 = \begin{pmatrix} 1 & 0 & 0 & 0 \\ 0 & 1 & 0 & 0 \\ 0 & 0 & 1 & 0 \\ 0 & 0 & 1 & 1 \end{pmatrix}^{-1} = \begin{pmatrix} 1 & 0 & 0 & 0 \\ 0 & 1 & 0 & 0 \\ 0 & 0 & 1 & 0 \\ 0 & 0 & 1 & 1 \end{pmatrix}, \quad (\text{B14})$$

and

$$S_3 R_3 = \begin{pmatrix} 1 & 0 & 0 & 1 \\ 0 & 1 & 1 & 0 \\ 0 & 1 & 0 & 0 \\ 1 & 0 & 0 & 0 \\ \hline 1 & 0 & 0 & 0 \\ 0 & 1 & 0 & 0 \\ 0 & 0 & 1 & 0 \\ 0 & 0 & 0 & 1 \end{pmatrix}. \quad (\text{B15})$$

Finally, we apply PHASE to qubits 1 and 2 so that

$$S_4 = Q_2 S_3 R_3 = \begin{pmatrix} 0 & 0 & 0 & 1 \\ 0 & 0 & 1 & 0 \\ 0 & 1 & 0 & 0 \\ 1 & 0 & 0 & 0 \\ \hline 1 & 0 & 0 & 0 \\ 0 & 1 & 0 & 0 \\ 0 & 0 & 1 & 0 \\ 0 & 0 & 0 & 1 \end{pmatrix}, \quad (\text{B16})$$

where

$$Q_2 = \begin{pmatrix} 1 & 0 & 0 & 0 & | & 1 & 0 & 0 & 0 \\ 0 & 1 & 0 & 0 & | & 0 & 1 & 0 & 0 \\ 0 & 0 & 1 & 0 & | & 0 & 0 & 0 & 0 \\ 0 & 0 & 0 & 1 & | & 0 & 0 & 0 & 0 \\ \hline 0 & 0 & 0 & 0 & | & 1 & 0 & 0 & 0 \\ 0 & 0 & 0 & 0 & | & 0 & 1 & 0 & 0 \\ 0 & 0 & 0 & 0 & | & 0 & 0 & 1 & 0 \\ 0 & 0 & 0 & 0 & | & 0 & 0 & 0 & 1 \end{pmatrix}. \quad (\text{B17})$$

S_4 is of the form of a graph state and represents the following Paulis:

$$\begin{aligned} \tilde{P}_1 &= X_1 I_2 I_3 Z_4, \\ \tilde{P}_2 &= I_1 X_2 Z_3 I_4, \\ \tilde{P}_3 &= I_1 Z_2 X_3 I_4, \\ \tilde{P}_4 &= Z_1 I_2 I_3 X_4. \end{aligned} \quad (\text{B18})$$

We now have

$$S'_{\text{start}} = Q^{-1} S_4 R^{-1}, \quad (\text{B19})$$

where

$$Q^{-1} := Q_1^{-1} Q_2^{-1} = \begin{pmatrix} 1 & 0 & 0 & 0 & | & 1 & 0 & 0 & 0 \\ 0 & 1 & 0 & 0 & | & 0 & 1 & 0 & 0 \\ 0 & 0 & 0 & 0 & | & 0 & 0 & 1 & 0 \\ 0 & 0 & 0 & 0 & | & 0 & 0 & 0 & 1 \\ \hline 0 & 0 & 0 & 0 & | & 1 & 0 & 0 & 0 \\ 0 & 0 & 0 & 0 & | & 0 & 1 & 0 & 0 \\ 0 & 0 & 1 & 0 & | & 0 & 0 & 0 & 0 \\ 0 & 0 & 0 & 1 & | & 0 & 0 & 0 & 0 \end{pmatrix} \quad (\text{B20})$$

and

$$R^{-1} := R_3^{-1} R_2^{-1} R_1^{-1} R_0^{-1} = \begin{pmatrix} 0 & 1 & 1 & 0 & 1 & 1 \\ 0 & 1 & 1 & 1 & 0 & 0 \\ 1 & 1 & 0 & 0 & 0 & 1 \\ 1 & 1 & 0 & 0 & 0 & 1 \end{pmatrix}. \quad (\text{B21})$$

The rotation circuit is shown in Fig. 4. Using Q^{-1} , S_4 and R^{-1} , we can work out that the phases for the six original operators are $(+1 +1 +1 -1 -1 -1)$. Therefore, we can construct measurements of the original Pauli strings as follows:

- P_1 from product of measurements of qubits 3 and 4,
- P_2 from product of measurements of qubits 1 to 4,

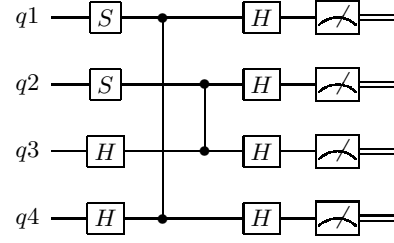


FIG. 4. The rotation circuit U for the CZ-construction walk-through example.

- P_3 from product of measurements of qubits 1 and 2,
- P_4 from the negative of measurement of qubit 2,
- P_5 from the negative of measurement of qubit 1,
- P_6 from the negative product of measurements of qubits 1, 3 and 4.

Appendix C: Proof of $O(kn/\log k)$

We prove the following Claim 2 via arguments of Patel, Markov, and Hayes [42]. As acknowledged in Ref. [42], these arguments originate from the ‘‘Method of Four Russians’’ [63]. Note that row operations correspond to CNOT gates, as explained in detail in Ref. [42].

Claim 2. *Let M be a $n \times n$ matrix with block form*

$$\begin{pmatrix} I_k & A \\ 0 & I_{n-k} \end{pmatrix}, \quad (\text{C1})$$

where A is any $k \times (n - k)$ matrix. Then $O(kn/\log k)$ row operations suffice to reduce M to identity I_n .

Proof. Let m be a constant we later choose. Partition A into $l := (n - k)/m$ consecutive column-blocks A_i , each containing m columns.

Start at A_1 and eliminate any duplicate rows using at most k row operations. There then remain at most 2^m unique rows in A_1 which can be eliminated by at most $m2^{m-1}$ row operations that add rows from I_{n-k} . A_1 is now zero.

For each of A_2, \dots, A_l perform the same operation as was done to A_1 . M then becomes

$$\begin{pmatrix} B & 0 \\ 0 & I_{n-k} \end{pmatrix}, \quad (\text{C2})$$

where B is some $k \times k$ matrix that must be invertible. B can then be row-reduced to I_k using $O(k^2/\log k)$ by the result of Ref. [42].

The total number N of row operations is therefore

$$N = (k + m2^{m-1}) \frac{n - k}{m} + O\left(\frac{k^2}{\log k}\right). \quad (\text{C3})$$

Choosing $m = \alpha \log k$, we find

$$N = \frac{k(n - k)}{\alpha \log k} + \frac{k^\alpha(n - k)}{2} + O\left(\frac{k^2}{\log k}\right), \quad (\text{C4})$$

which is $O(kn/\log k)$ provided $\alpha < 1$. \square

Appendix D: Example to demonstrate that combining two groups into one reduces R

Consider the example in Ref. [3, 23] where we consider measuring the energy, given by Hamiltonian

$$H = -XX - YY + ZZ + IZ + ZI \quad (\text{D1})$$

on the state $|\psi\rangle = |01\rangle$. For these Paulis, the covariance matrix is

$$C = \begin{pmatrix} 1 & 1 & 0 & \mathbf{0} & \mathbf{0} \\ 1 & 1 & 0 & \mathbf{0} & \mathbf{0} \\ 0 & 0 & 0 & 0 & 0 \\ \mathbf{0} & \mathbf{0} & 0 & 0 & 0 \\ \mathbf{0} & \mathbf{0} & 0 & 0 & 0 \end{pmatrix}. \quad (\text{D2})$$

The covariance between the non-commuting operators in the upper right and lower left blocks is not defined. We have set them to equal zero for convenience (highlighted in bold).

First, we consider grouping the Paulis into

$$\{-XX, -YY, ZZ\}, \{IZ, ZI\}. \quad (\text{D3})$$

For these groups of Paulis, the coefficient vectors are given by

$$\mathbf{a} = \begin{pmatrix} -1 \\ -1 \\ 1 \\ 0 \\ 0 \end{pmatrix}, \quad \mathbf{c} = \begin{pmatrix} 0 \\ 0 \\ 0 \\ 1 \\ 1 \end{pmatrix}. \quad (\text{D4})$$

The number of measurements to achieve an accuracy of ϵ is

$$\begin{aligned} M_g &= \frac{1}{\epsilon^2} \left(\sqrt{\mathbf{a}^\dagger C \mathbf{a}} + \sqrt{\mathbf{c}^\dagger C \mathbf{c}} \right)^2 \\ &= \frac{1}{\epsilon^2} \left(\sqrt{4} + \sqrt{0} \right)^2 \\ &= \frac{4}{\epsilon^2}. \end{aligned} \quad (\text{D5})$$

Now, let us consider breaking up the first group into

$$\{-XX\}, \{-YY, ZZ\}. \quad (\text{D6})$$

In this case, the coefficient vectors are

$$\mathbf{a} = \begin{pmatrix} -1 \\ 0 \\ 0 \\ 0 \\ 0 \end{pmatrix}, \quad \mathbf{b} = \begin{pmatrix} 0 \\ -1 \\ 1 \\ 0 \\ 0 \end{pmatrix}, \quad \mathbf{c} = \begin{pmatrix} 0 \\ 0 \\ 0 \\ 1 \\ 1 \end{pmatrix}. \quad (\text{D7})$$

The number of measurements required to attain an accuracy ϵ is therefore

$$\begin{aligned} M_g &= \frac{1}{\epsilon^2} \left(\sqrt{\mathbf{a}^\dagger C \mathbf{a}} + \sqrt{\mathbf{b}^\dagger C \mathbf{b}} + \sqrt{\mathbf{c}^\dagger C \mathbf{c}} \right)^2 \\ &= \frac{1}{\epsilon^2} \left(\sqrt{1} + \sqrt{1} + \sqrt{0} \right)^2 \\ &= \frac{4}{\epsilon^2}. \end{aligned} \quad (\text{D8})$$

Therefore, under the optimal measurement strategy it is not preferable to break the $\{-XX, -YY, ZZ\}$ group into $\{-XX\}$ and $\{-YY, ZZ\}$. In this specific example we have equality because for $\alpha = -\beta$ we have $\langle \alpha \mathbf{a} + \beta \mathbf{b}, \alpha \mathbf{a} + \beta \mathbf{b} \rangle = 0$.

Appendix E: Derivation of \hat{R} formula

Claim 3. For R as defined in Eq. (19), if all variances and covariances are replaced with their expectation value over uniform spherical distribution, we obtain a new metric, \hat{R} , given by

$$\hat{R} = \left(\frac{\sum_{i=1}^N \sum_{j=1}^{N_i} |a_{ij}|}{\sum_{i=1}^N \sqrt{\sum_{j=1}^{N_i} a_{ij}^2}} \right)^2. \quad (\text{E1})$$

Proof. The variance of a single Pauli operator is

$$\text{Var}[P_i] := 1 - \langle P_i \rangle^2. \quad (\text{E2})$$

The expectation of this variance for all $P_i \neq I$ is

$$\begin{aligned} \mathbb{E}[\text{Var}P_i] &= 1 - \mathbb{E}[\langle P_i \rangle^2] \\ &= 1 - \int [|\langle \psi | P_i | \psi \rangle|^2] d\psi \\ &= 1 - \alpha_n, \end{aligned} \quad (\text{E3})$$

where $\alpha_n := 1/(2^n + 1)$, with n the number of qubits, is independent of P_i [54, Exercise 7.3]. Trivially, $\text{Var}[I] = 0$. In addition, it was shown in Ref. [23] that

$$\mathbb{E}[\text{Cov}[P_i, P_j]] = 0, \quad (\text{E4})$$

for all $P_i \neq P_j$. Simple substitution of these results yields Eq. (E1). \square

Appendix F: Full numerical results

In this Appendix, we present the results of the numerical simulations discussed in the main text.

Molecule	n qubits	t Paulis	Grouping			Ratios R, \hat{R}				Rotation Circuit $2q$ -size		
			N	$\overline{m_i}$	$\overline{k_i}$	R min	R mean	R max	\hat{R} mean	max theory	max true	mean
H ₂	2	4	2	2.00	1.50	1.09	1.93	4.60	1.76	0	0	0
H ₃ ⁺	4	59	10	5.90	3.50	3.76	11.92	33.04	10.25	6	3	0.80
LiH	10	630	41	15.37	6.85	19.60	24.91	34.74	23.97	45	18	5.29
OH ⁻	10	630	38	16.58	7.29	6.32	8.90	12.86	8.51	45	17	5.63
HF	10	630	39	16.15	6.97	6.07	8.57	12.27	8.21	45	16	5.74
H ₂ O	12	1085	51	21.27	9.04	7.68	11.27	16.96	10.67	66	26	7.37
BH ₃	14	1584	66	24.00	10.36	17.21	20.93	32.13	20.05	91	26	9.56
NH ₃	14	3608	118	30.58	11.34	12.65	15.96	26.93	15.31	91	28	10.26
CH ₄	16	3887	123	31.60	13.39	16.96	21.63	29.33	20.27	120	45	16.75
O ₂	18	2238	67	33.40	13.48	-	-	-	20.23	153	44	21.57
N ₂	18	2950	78	37.82	13.91	-	-	-	22.10	153	53	20.42
CO	18	4426	128	34.58	13.48	-	-	-	21.31	153	50	20.23
HCl	18	4538	123	36.89	13.87	-	-	-	10.36	153	49	20.35
NaH	18	5850	135	43.33	14.73	-	-	-	12.90	153	45	21.44
H ₂ S	20	6277	147	42.70	16.06	-	-	-	11.60	190	58	25.98
PH ₃	22	19746	304	64.95	18.77	-	-	-	13.05	231	67	28.02
SiH ₄	24	18713	304	61.56	20.98	-	-	-	13.94	276	77	36.03
NaF	26	16538	287	57.62	20.44	-	-	-	23.36	325	90	42.28
LiCl	26	17044	292	58.37	20.46	-	-	-	12.22	325	89	39.42
KH	26	24290	325	74.74	22.30	-	-	-	12.87	325	115	45.18
CO ₂	28	11429	216	52.91	21.02	-	-	-	38.47	378	104	44.51
F ₂ O	28	20541	317	64.80	22.83	-	-	-	36.82	378	105	46.12
NO ₂	28	20549	311	66.07	22.93	-	-	-	40.69	378	109	46.25
Cl ₂	34	34334	378	90.83	28.09	-	-	-	26.58	561	156	73.24
NaCl	34	42826	498	86.00	28.54	-	-	-	20.46	561	166	74.34
SF ₂	36	56025	567	98.81	31.96	-	-	-	30.65	630	180	78.67
HBr	36	62589	602	103.97	31.88	-	-	-	16.03	630	154	78.98
SO ₂	36	75315	691	108.99	33.21	-	-	-	29.75	630	187	66.90
NO ₃ ⁻	38	61132	622	92.28	31.23	-	-	-	65.01	703	182	86.40
H ₂ Se	38	69684	631	110.43	33.91	-	-	-	16.49	703	196	86.88

TABLE IV. The full set of results of the numerical simulations discussed in the main text, with molecules as listed. The molecular geometry is approximately that of the equilibrium configuration. For each molecule, we show a number of results related to the grouping of Hamiltonian terms, how the grouping reduces the number of measurements required, and the number of two-qubit gates in the resulting rotation circuits. In all cases, we used OpenFermion [57] and Psi4 [64] to obtain Hamiltonians in the STO-3G basis and under the symmetry conserving Bravyi-Kitaev transformation [17, 58]. Using the grouping method described in the text, SORTED INSERTION, the number of groups, N , the average number of terms per group, $\overline{m_i}$, and the average rank of the groups, $\overline{k_i}$ are shown, for molecules with n qubits and t Pauli operators, excluding the identity, in the Hamiltonian sum. Given the groupings shown, for the smallest nine molecules, we calculated the ratio R , as given in Eq. (19), for 100 randomly selected trial states, prepared by choosing random sets of parameters for a hardware efficient ansatz preparation circuit of depth 1. For each molecule, we show the mean, minimum and maximum values of R obtained from the 100 runs. We also show the value of \hat{R} , given by Eq. (29) obtained, which we can see is close in value to the mean value of R where this has been calculated. A key result of interest is the maximum number of two-qubit gates required to obtain a measurement of all the operators in a given Hamiltonian. We show the theoretical maximum, given by the largest value of $kn - \frac{1}{2}k(k+1)$ for any group, and the true largest value for any group once the rotation circuits have been found. The ratio of these two numbers is shown in Fig. 3(c), and we can see it has a value of approximately 3.5. We also show the mean number of two-qubit gates required in a rotation circuit, averaged across all groups for a given molecule.